Zilstra, A., & Johnson, D. A. "A Novel Acoustic Feedback Mechanism Originating From Within the Laminar Separation Bubble," AIAA 2026-3211. 32nd AIAA/CEAS Aeroacoustics Conference (2026). May 2026. https://doi.org/10.2514/6.2026-3211

A Novel Acoustic Feedback Mechanism Originating from within the Laminar Separation Bubble

Alison Zilstra * and David A. Johnson†
University of Waterloo, Waterloo, Ontario, N2L 3G1, Canada

A computational aeroacoustic analysis of tonal noise generated by a laminar separation bubble (LSB) in close proximity to the airfoil trailing edge (TE) is completed through the study of the SD 7037 airfoil at the Reynolds number, Re, of 4.1×10^4. Analysis of the boundary layer transition uncovered a new feedback mechanism originating from within the suction side LSB caused by the lift-off and subsequent touchdown of the Kelvin-Helmholtz (K-H) rolls. The numerical methods used are incompressible wall-resolved Large Eddy Simulation (LES) and the Ffowcs-Williams and Hawkings (FW-H) acoustic analogy, and results are validated against aerodynamic and aeroacoustic experiments. The simulation accurately predicts amplified tonal noise at 1° angle of attack and the tonal noise source is identified as the K-H rolls shedding past the airfoil TE. The LSB feedback mechanism is found to operate independently from the TE acoustic feedback typically discussed for tonal noise amplification. An estimation of the interference between the TE acoustic feedback and the LSB feedback predicts constructive interference which is consistent with the further amplification of the tonal noise seen in the validating acoustic measurements. The analysis shows that K-H rolls in the LSB are both the source of the tonal noise generated at the TE and a mechanism of feedback originating from within the LSB.

I. Introduction

Tonal airfoil self-noise is generated from the interaction of the boundary layer (BL) and the sharp trailing edge (TE) of the airfoil [1]. Low Reynolds number (Re) airfoils, which operate at a chord based Re of less than 5×10^5, are used in applications including compressor cascades of aircraft engines, small wind turbines, and the wings or rotors of micro air vehicles. Low Re airfoils often generate problematic tonal noise due to the flow structures present as the BL transitions to turbulence [2]. When operating at a modest Re of less than 1×10^5, the airfoils in these applications are capable of producing loud tonal noise due to the elongated chordwise length of a laminar separation bubble (LSB) that forms in the BL in close proximity to the airfoil TE [3]. Under these conditions, the tonal noise generated by an airfoil is amplified through acoustic feedback [4] which alters the frequencies of the BL transition structures. The reduction of the tonal noise generated by low Re airfoils requires an improved understanding of the complexities of the BL structures that generate tonal noise and their interaction with the acoustic feedback process.

The airfoil self-noise mechanism responsible for tonal noise generation is the laminar BL-vortex shedding (LBL-VS) mechanism for which the noise source is the TE vortex shedding [1]. However, the regular frequency structures at the TE can originate from within a transitional BL or in a LSB [5]. When a LSB develops in close proximity to the TE for low Re airfoils, several experimental works have shown that the Kelvin-Helmholtz (K-H) rolls that form in the LSB are often responsible for the tonal TE noise [2, 3, 6–9]. The tonal noise is amplified through a proposed acoustic feedback process [1] or acoustic coupling [5, 10] and many feedback loops have been proposed [1, 4, 11–15] with the overarching concept illustrated in Figure 1 based on the description by Longhouse [13].

The acoustic feedback process is said to "lock" the frequency of the BL transition structures onto the tonal noise frequency in a positive feedback loop. The acoustic pressure waves travelling upstream from the TE interact with the laminar BL which is susceptible to excitation of Tollmien-Schlichting (T-S) waves at a range of frequencies [16]. This process may amplify numerous T-S wave frequencies depending on the phase shift between the two locations [17], and the amplified T-S waves propagate downstream in the BL and result in BL transition structures with an amplified pressure fluctuation at the TE. In the case of a LSB, the amplified T-S waves develop into K-H rolls at the same frequency which in turn generate amplified tonal noise from their interaction with the airfoil TE. A method for the calculation of the amplified tone frequencies from TE acoustic feedback was proposed by Kingan and Pearse [17], where the total

*Postdoctoral Researcher, Wind Energy Group, Mechanical and Mechatronics Engineering, 200 University Ave W and AIAA Member 976029
†Professor, Wind Energy Group, Mechanical and Mechatronics Engineering, 200 University Ave W

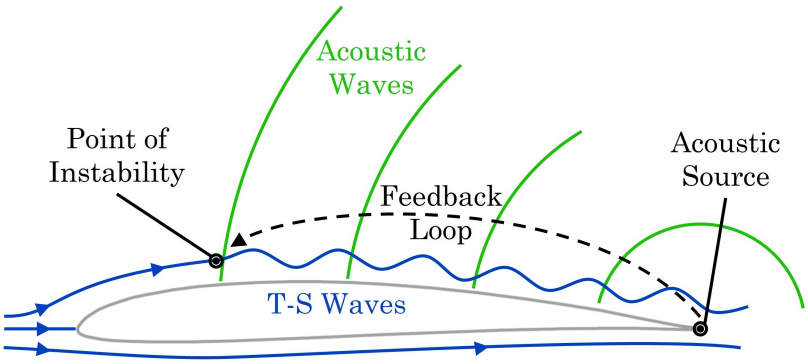


Fig. 1 Acoustic feedback loop diagram for tonal TE noise

phase shift between the initial T-S instability and the returning acoustic wave are calculated to determine if feedback will occur at a given tonal noise frequency.

The study of tonal airfoil self-noise and acoustic feedback using computational aeroacoustics (CAA) methods requires a computational fluid dynamics (CFD) method that is able to accurately capture the details of the transient behaviour of the structures in the BL transition, including the K-H rolls formed in the LSB. Several validated CAA studies of airfoil self-noise have successfully employed direct CAA [18–21] and acoustic analogies [10] to predict the LSB and related tonal noise from low Re cambered airfoils. Notably, studies of the CD airfoil [18–20] have identified the LSB as a source of tonal noise separate from the TE noise at high angles of attack (AOA) when the LSB is located near the airfoil LE. Deuse and Sandberg [18] and Arroyo Ramo *et al.* [19] found that tonal noise from the LSB was detected at the far-field receiver, however this was due to the downstream convection of the LSB pressure fluctuations to the TE and their contribution to the TE noise source. Wu *et al.* [20] found that the FW-H analogy did not predict propagation of the LSB tonal noise to the far-field receiver and therefore was a near-field source of tonal noise.

This numerical study examines a cambered low Re airfoil at a modest Re which has an elongated LSB and is known to generate tonal noise at low AOAs. The simulations are completed using incompressible wall-resolved large eddy simulation (LES) and the Ffowcs-Williams and Hawkings (FW-H) acoustic analogy and the results are thoroughly validated against experimental data. The present study is an expansion of the prior detailed time-averaged validation of the LSB simulation [22], transient study of the LSB [23] and the preliminary aeroacoustic validation [24] which identified amplified tonal noise at 1° AOA that was not dominant at higher AOAs. The amplified tonal noise at 1° AOA predicted in the prior numerical studies occurs in the absence of TE acoustic feedback since the incompressible simulation method does not capture this effect and recent findings of the transient study of the LSB [23] identified a novel feedback mechanism originating from within the LSB. The current study examines the transient aerodynamics of the LSB to gain a deeper understanding of the LSB as a source of tonal noise and the role of the novel LSB feedback mechanism as a separate source of feedback from the established TE mechanism.

II. Methodology

The simulations were performed using ANSYS Fluent, release 22.2, with wall-resolved LES as the CFD model and FW-H as the acoustic analogy. The selected airfoil profile is the SD 7037 airfoil [25, 26] which is a cambered airfoil designed for low Re applications and the geometry details are summarized in Table 1. The simulations are performed at a Re of 4.1×10^4 with a chord length, c, of 25.8 mm for which there is experimental data available for the validation of the aerodynamic [27] and aeroacoustic [28] behaviours. The aeroacoustic experiments measured the noise from a microphone located $3.0c$ below the quarter-chord of the airfoil [28] and the receiver location for the FW-H analogy was set at the same location. The wall-resolved LES was completed using the dynamic Smagorinsky-Lilly sub-grid scale (SGS) model and the simulation method has been thoroughly validated in prior study for the time-averaged prediction of the LSB [22]. The mass and momentum conservation equations were solved in the incompressible form since the direct simulation of acoustic wave propagation using a compressible simulation is both computationally expensive [29] and not required for the use of the FW-H acoustic analogy. The incompressible wall-resolved LES simulation method therefore does not include the TE acoustic feedback effect, however it has been shown in the preliminary aeroacoustic study to predict the tonal noise without the influence of the TE feedback [24].

Table 1 Geometry and numerical details

Airfoil Profile		SD 7037	Span	b	$0.2c$
Reynolds Number	Re	4.1×10^4	Radius	R	$12c$
Chord	c	0.0258 m	Downstream Length	L	$12c$
Inflow Velocity	U_∞	23.8 m/s	Number of Elements		4.5×10^6
Inflow Turbulence	Tu	1%	Chordwise, Spanwise Divisions		300, 50
Angle of Attack	α	1°	Wall First Layer Height		5×10^{-6} m
Time Step	Δt	2×10^{-6}	Wall-Normal Expansion		1.1

The simulations were run using 128 cores on a high performance compute cluster in the Digital Research Alliance of Canada network [30] and collected 118 chord-based mean flow residence times (MFRT) of data (0.128 s) at a time step, Δt, of 2×10^{-6} s. The initial portion of the acoustic signal was truncated to remove the transient numerical effects from the initialization of the simulation, resulting in a signal length of 0.10 s (92 MFRT). The development of the BL transition structures are measured using the pressure and velocity signals from 126 measurement probes placed in the BL at chordwise spacings of $0.05c$ and at a wall-normal distance from the airfoil surface of $3 \times 10^{-2}c$ and $4 \times 10^{-3}c$. The signals were collected for 1×10^4 time steps, which is a total time of 0.02 s (18 MFRT). The global x,y,z-coordinates are converted to s,n,z-coordinates where the s-velocity, U_s, is tangent to the local airfoil curvature and the n-velocity is normal to the curvature.

A. Domain Geometry and Mesh

The fluid domain surrounding the airfoil is a C-mesh as shown in Figure 2(a) and the radius, R, and downstream length, L, dimensions of the domain can be found in Table 1. The spanwise length of the domain, b, was set at a length of $0.2c$ and is consistent with high-fidelity simulations of a LSB over symmetric NACA airfoils [31, 32] and cambered airfoils [33–35]. The boundary conditions used for the simulation domain are included in Figure 2(a). The spanwise boundary condition is set as a periodic boundary condition which is commonly used for simulations of low Re transitional separated flow with a spanwise extent of $0.2c$ [31–35]. The spanwise extent and spanwise boundary condition are of greater concern for compressible CAA simulations, which requires the development and propagation of spanwise acoustic waves [36]. The current simulations generate the aeroacoustic prediction through incompressible LES with an acoustic analogy and therefore the current selection of the periodic boundary condition will not introduce any problematic spanwise aeroacoustic patterns.

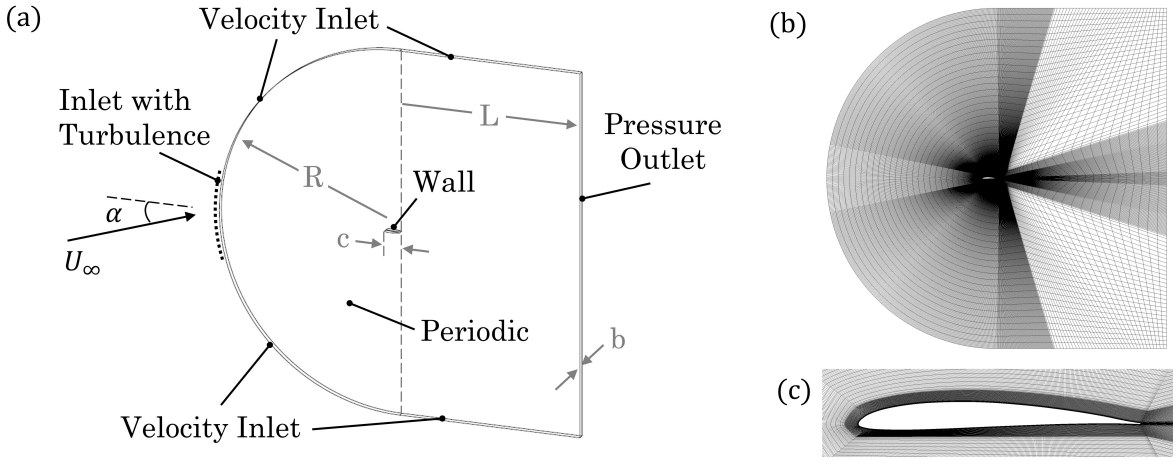


Fig. 2 (a) Computational domain geometry and boundary conditions. Mesh distribution for (b) full domain and (c) close-up of airfoil

The structured hexahedral mesh is shown in Figure 2 (b) and (c) and the mesh distribution in the airfoil BL is strictly controlled to ensure adequate resolution for the wall-resolved LES method. The SGS filter length, Δ, is calculated as the cubed root of the cell volume [37] and turbulence of length scales smaller than the filter length will be calculated by the SGS model. The mesh for the airfoil BL shown in Figure 2(c) was generated through the application of a viscous lengthscale filter length criterion in the regions of attached BL and a free-shear filter length criterion for the regions with a separated BL in the LSB. The details of the filter length criteria are included in the prior study on the transient LSB [23] and the sensitivity of the tonal noise prediction to the filter length at 1° AOA as well as 3° and 5° AOA are included in the preliminary aeroacoustic study [24]. The details of the resulting mesh distribution at the airfoil surface are summarized in Table 1.

III. Results

A. Validation and Tonal Noise Source

The validation of the LSB simulation is completed through a comparison of the time-averaged suction side pressure coefficient, C_p, with experimental PIV data [27] in Figure 3(a). The 1° AOA simulation is a complex low Re case where there is laminar BL separation with a transitional BL at the TE, rather than a fully-formed LSB with a time-averaged reattachment location. The chordwise pressure gradient is in agreement with the experimental data and the chordwise location of BL separation, x_s, determined using the skin friction coefficient, C_f, is at $x_s/c = 0.55$ [23]. The time-averaged BL transition, x_{tr}, is at the location of the maximum shape factor, H, of the BL velocity profiles [38, 39] and the simulations predict a location of $x_{tr}/c = 0.925$ which agrees closely with the experimental location of $x_{tr}/c = 0.91$ [23]. The incompressible wall-resolved LES method is able to accurately predict the location of the LSB and the close proximity of x_{tr} to the TE indicates that K-H rolls formed within the LSB will interact with the TE to generate tonal noise.

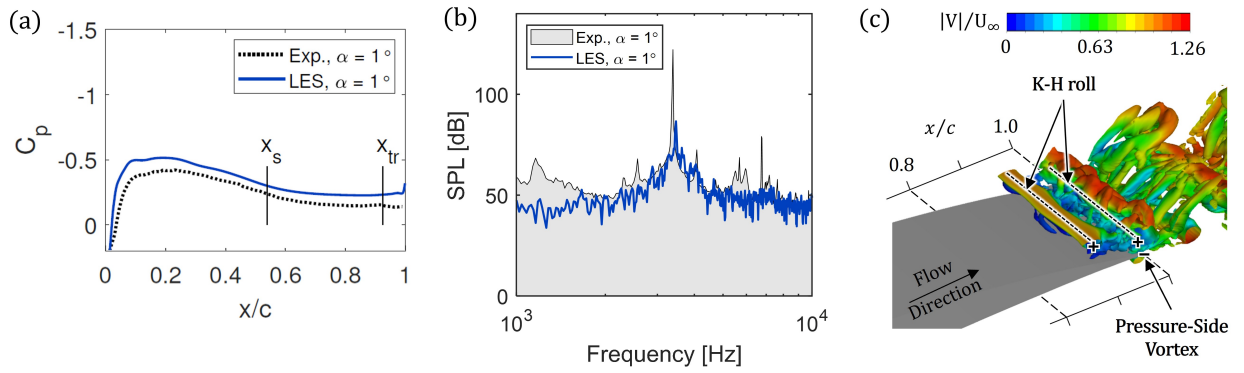


Fig. 3 (a) Suction side pressure coefficient compared with experimental measurements [27] and labelled locations of BL separation, x_s, and transition, x_{tr}. (b) Acoustic SPL spectrum compared with experimental spectrum [28]. (c) TE Q-Criterion iso-surface of $5 \times 10^7\ s^{-2}$ with "+" at core of clockwise rotating K-H roll and "-" at core of counter rotating vortex

The narrowband acoustic spectrum predicted by the FW-H acoustic analogy is shown in Figure 3(b) and is validated through comparison with the measured experimental spectrum [28] for the narrowband frequency range of 1 kHz to 10 kHz. The simulation predicts a tonal noise frequency, f_{tone}, of 3.47 kHz and sound pressure level (SPL) of 86.6 dB and the predicted tone is in excellent agreement with the experimental tone at a frequency of 3.39 kHz and an SPL of 122.2 dB. The under-prediction of the tonal noise SPL is expected when considering that the incompressible simulation method omits the TE feedback mechanism, however, the tonal noise is amplified by the novel LSB feedback mechanism which will be discussed in the later sections of this paper. The simulated and experimental spectra both contain a broadband hump of elevated SPL that is centred on f_{tone} ranging from approximately 2 kHz to 4.5 kHz and indicates the range of T-S wave frequencies to which the laminar BL is naturally susceptible. The accuracy of the tonal noise prediction combined with the aerodynamic analysis fully validates the method of incompressible wall-resolved LES and FW-H acoustic analogy for prediction of tonal noise generated by a low Re airfoil with a LSB in close proximity to the

TE. The high confidence in the accuracy of the transient simulation gained through the validation process serves as the foundation for the analysis in the remainder of the paper which investigates the tonal noise source and the influence of the TE and LSB feedback mechanisms on tonal noise amplification.

The source of the tonal noise is determined through an examination of the coherent structures in the BL at the TE, which is visualized using Q-criterion iso-surfaces in Figure 3(c). The instantaneous Q-criterion iso-surface is at a value of $5 \times 10^7\ s^{-2}$ with the flow direction from lower left to upper right and the surface is coloured with the non-dimensional velocity magnitude $|V|/U_\infty$ to highlight the height and shape of the structures. The K-H rolls labelled in Figure 3(c) are clockwise-rotating spanwise structures that pinch-off from the reverse flow region of the LSB and their interaction with the TE results in the generation of a counter-rotating vortex from the pressure side BL. The formation of the K-H rolls and their interaction with the TE is summarized in the diagram in Figure 4. The K-H rolls have low gauge pressure and therefore the entire span of the airfoil TE has a synchronized fluctuation between low and high pressure as the suction side K-H rolls are shed into the wake. Since the sharp TE of the airfoil is an efficient scattering centre of acoustic energy [40], the spanwise synchronization of the pressure fluctuations from the K-H rolls results in tonal noise of a high SPL at the dominant K-H roll frequency, f_{KH}. A spectral analysis of the U_s measured from the 126 measurement probes is used to identify f_{KH} as 3.45 kHz and confirms the K-H rolls as the source of the TE tonal noise due to the similarity of the dominant f_{KH} to the simulated f_{tone} of 3.47 kHz. This finding is consistent with prior experimental [2, 3, 6–8] and numerical [21] studies of low Re airfoils with a LSB near the TE, where K-H rolls present due to a suction side and/or pressure side LSB have been previously shown to be the source of the TE tonal noise.

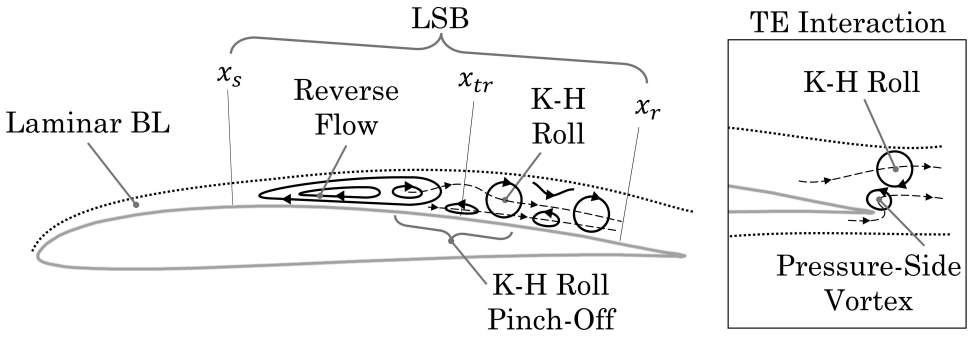


Fig. 4 Diagram of the transient development of the LSB and details of K-H roll interaction with the TE. Dashed lines show path of vortex cores

B. LSB Feedback Mechanism

The dominance of f_{KH} in the simulated BL occurs in the absence of the TE acoustic feedback and therefore an examination of the transient formation of the K-H rolls is completed to determine the source of the dominant frequency behaviour. Gauge pressure, P, contours at time intervals of 1×10^{-4} s are shown in Figure 5(a), (b) and (c) which focus on the behaviour of a newly formed K-H roll passing x_{tr} at $0.925c$. The K-H roll being tracked is indicated with a circle and a plus sign located at the K-H roll core, while the non-tracked K-H rolls are also indicated with a plus sign. In Figure 5(a), the new K-H roll pinches off from the reverse flow region of the LSB and the pinch-off behaviour forms a thin, counter-rotating vortex at the wall between the new K-H roll and the reverse flow region. This counter-rotating vortex is shown in Figure 4 at x_{tr} and the counter-rotating vortex cores are marked with a negative sign in the pressure contours in Figure 5(a), (b) and (c). The K-H roll pinch-off behaviour occurs consistently with time and the paths of the K-H roll and counter-rotating vortex cores are included in Figure 4.

As the K-H roll propagates downstream, the velocity magnitude at the outer circumference of the new K-H roll increases and the gauge P at the centre of the K-H roll decreases. At x_{tr}, the wall-normal distance of the K-H roll core increases as is shown in Figure 5(a) and (b), and this increase in wall-normal distance of the K-H roll will be referred to as K-H roll lift-off. After the core of the K-H roll passes x_{tr}, the wall-normal distance of the core reduces which is seen in Figure 5(c). The decrease in the wall-normal distance of the K-H roll causes an interaction between the newly formed roll and the airfoil surface, which will be referred to as K-H roll touchdown. The K-H roll touchdown, which occurs at $x_{TD}/c = 0.98$, results in a noticeable decrease in the gauge pressure for $x/c \leq 0.85$, labelled F in Figure 5(c), and is evidence of an upstream pressure feedback occurring due to the K-H roll touchdown in the LSB.

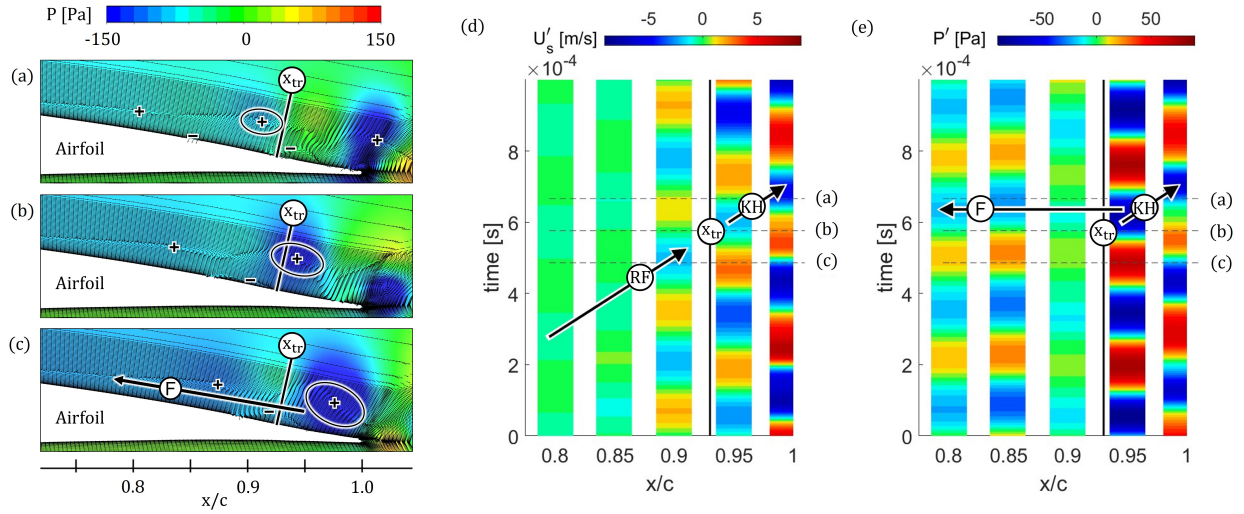


Fig. 5 Representative K-H roll gauge P contours with constant length velocity vectors for $0.725 < x/c < 1.05$ annotated to indicate dominant structures for K-H roll (a) pinch-off, (b) lift-off and (c) touchdown. Filtered signals of (d) U_s' and (e) P' at probe x/c locations vs. time and wall-normal distance $4 \times 10^{-3}c$.

The feedback is examined quantitatively using the U_s and gauge P signals from the BL probes shown in Figure 5(d) and (e) for the chordwise range of $0.8 \leq x/c \leq 1$. The probe sampling frequency of 500 kHz is sufficiently high to track the chordwise progression of individual U_s and P fluctuations associated with the BL transition and K-H roll formation. A graphical method was employed to visually track the fluctuations measured by the probes rather than applying statistical methods typically used for experimental data with a lower sampling frequency or lower spatial resolution such as cross-correlations or quadrant analysis. This visual method of analysis focuses on the flow structures which develop at frequencies nearest to the dominant f_{KH} of 3.45 kHz and therefore a bandpass filter was applied to each signal from 1 kHz to 10 kHz to remove low frequency oscillation and higher frequency content. The filtering of frequencies below 1 kHz performs a similar function to subtracting the mean from the signal to extract the fluctuating component and therefore the filtered signals are referred to as U_s' and P' in this analysis.

A K-H roll is tracked in Figure 5(d) and (e) using black arrows through the reverse flow region of the LSB, labelled RF, and the region of fully-formed K-H rolls, labelled KH. The BL probes are positioned between the core of the K-H roll and the wall which results in a negative U_s' fluctuation occurring when a K-H roll passes the probe due to the clockwise rotation. The representative gauge P contours in Figure 5(a)-(c) are from simulation time steps that do not directly correspond to the U_s' and P' signals, however the positioning of the K-H rolls and counter-rotating vortices aligns with the signals due to the consistency of the transient K-H roll formation. The K-H roll marked in Figure 5(a)-(c) with a circle is representative of the K-H roll being tracked in Figure 5(d) and (e) and the horizontal dotted lines in Figure 5(d) and (e) are the times in the U_s' and P' signals which align with the K-H roll and counter-rotating vortices positioning.

The pressure feedback identified in Figure 5(c) is also shown in the negative P' fluctuation labelled F in Figure 5(e), which occurs simultaneously with the K-H roll touchdown at $x_{TD}/c = 0.98$. The pressure feedback occurs consistently with time, as is shown by the alternating positive and negative P' fluctuation with a duration of 0.15×10^{-3} s for the P' signals at $0.8c$ and $0.85c$. The pressure feedback travels in the chordwise direction towards the LE through the reverse flow region of the LSB and the attached laminar BL with an approximate magnitude of 20 Pa at $0.85c$ and reducing to 2.5 Pa at $0.025c$. For $x/c < 0.8$, the U_s' signals also capture an alternating positive and negative fluctuation of approximately 0.05 m/s, or $0.0015U_\infty$, which occurs for a duration of 0.15×10^{-3} s. The amplitude of the U_s' fluctuation is comparable to the experimental U_s' amplitude of T-S waves for a flat plate BL transition measured at 0.3% to 1% of the free-stream velocity [41, 42]. When compared to the time evolution of the P' fluctuations in the laminar BL, the LSB feedback is found to induce an anti-correlated U_s' fluctuation similar to a T-S wave at a time lag of 0.06×10^{-3} s. The positive feedback loop therefore operates in the same manner as the TE acoustic feedback shown in Figure 1 where the T-S waves lock on to the K-H roll frequency such that a single frequency dominates the velocity and pressure fluctuations in the transitional BL. Further evidence of the LSB feedback initiating T-S waves in the laminar BL is

included in the prior transient study of the LSB [23] where the intermittency of the LSB feedback at 5° AOA shows the contrast between T-S wave formation with and without the LSB feedback effect.

The novel LSB feedback mechanism initiated by the K-H roll touchdown has not been previously reported in transient studies of LSB formation. However, the finding of the LSB as a source of feedback is in agreement with the recent findings of the LSB as a source of tonal noise separate from the tonal TE noise [18–20] and the current study identifies the source of this pressure feedback as the K-H roll touchdown in the LSB. The feedback effect is only identifiable in the present study due to the high sampling frequency of the BL probes and the high confidence in the simulation results due to the validation of both the time-averaged LSB and the tonal noise prediction.

C. LSB and TE Feedback Interference

The simulations have been shown to capture LSB feedback originating from the K-H roll touchdown while omitting the separate TE feedback mechanism originating from the tonal noise generated from the K-H roll interaction with the TE. Determining the total effect of the feedback on the tonal noise amplification requires an estimation of the constructive or destructive interference between the pressure waves from the separate LSB and TE feedback sources. The combined effect of the feedback is illustrated in Figure 6 which is a modified version of the transient LSB development diagram shown in Figure 4. Upstream of x_{tr}, the TE feedback, shown in green, and the LSB feedback, shown in red, travel upstream as a combined source of feedback which under the assumption of linear superposition will together alter the development of the T-S wave frequencies in the laminar BL. The interference between the TE and LSB feedback is determined using the phase difference between the two feedback mechanisms at the downstream end of the combined feedback region, which is the time-averaged x_{tr} of $0.925c$.

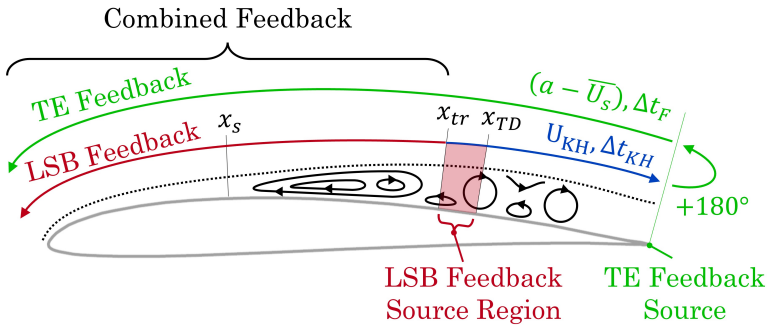


Fig. 6 Diagram for estimation of interference of LSB feedback and TE feedback

The method of this interference calculation is a modified version of the theoretical method proposed by Kingan and Pearse [17], which predicts the phase difference between the T-S waves and the TE feedback at the chordwise location of T-S wave initiation. The estimation is completed for a specific f_{tone} and accounts for the downstream propagation time of the T-S waves, the 180° phase shift of the dipole acoustic source at the TE, and the upstream propagation time of the acoustic waves. In the current work, the same method is used to determine the phase difference between the K-H rolls and the TE feedback at x_{tr}, the source location of the LSB feedback, using the variables defined in Figure 6. The LSB feedback is represented by a pressure fluctuation, $P = \sin(2\pi f_{tone} t)$. The TE feedback is represented by $P = -\sin(2\pi f_{tone}(t - \Delta t_{KH} - \Delta t_F))$, where the 180° phase shift is applied by multiplying by -1.

The propagation times Δt_{KH} and Δt_F are determined from the U_s measured by the BL probes which capture a constant K-H roll convection velocity of $U_{KH} = 13.0 m/s$ and an average U_s between x_{tr} and the TE of $\bar{U}_s = -1.4 m/s$ at a wall-normal height of $4 \times 10^{-3} c$. The analysis predicts constructive interference of the LSB and TE feedback mechanisms with a phase shift of 0.05π. Constructive interference of the feedback is consistent with the higher tonal noise SPL of 122.2 dB in the experimental measurements, which includes tonal noise amplification from both feedback mechanisms, in comparison to the lower SPL of 86.6 dB of the simulated tone where only the LSB feedback is present. The interference estimation is sensitive to the positioning of x_{tr} relative to the TE with changes of $\pm 0.05c$ resulting in destructive interference of the LSB and TE feedback mechanisms with phase shifts of 0.63π to 0.72π. The simulation of the interference of the LSB and TE feedback mechanisms in compressible CAA simulations therefore requires significant attention to the chordwise positioning of the LSB, and particularly the time-averaged x_{tr} which is the source of the LSB feedback.

IV. Conclusion

A numerical study of the tonal noise generated by the SD 7037 airfoil at low Re was completed using incompressible wall-resolved LES and the FW-H acoustic analogy. The validated results for the aerodynamic and aeroacoustic behaviour of the airfoil at 1° AOA show that a suction side LSB at the TE is the source of tonal noise due to the shedding of K-H rolls past the TE. The K-H rolls were shown to lift-off and touchdown shortly after formation in the LSB, and resulted in a pressure feedback which is independent from the TE feedback caused by the tonal TE noise. The LSB feedback is also shown to constructively interfere with the estimated TE feedback, and shows the importance of capturing this new feedback mechanism in the CAA analysis of low Re airfoils with a LSB. The novel LSB feedback mechanism and its interaction with the TE feedback mechanism is a significant advancement in the understanding of the amplification tonal airfoil self-noise and is a previously missing factor in the aeroacoustic design for numerous low Re applications where airfoils operate with a LSB in close proximity to the airfoil TE.

References

[1] Brooks, T. F., Pope, D. S., and Marcolini, M. A., "Airfoil self-noise and prediction," Tech. Rep. NASA-RP-1218, NASA Reference Publication, 1989. http://ntrs.nasa.gov/archive/nasa/casi.ntrs.nasa.gov/19890016302.pdf.

[2] Pröbsting, S., Serpieri, J., and Scarano, F., "Experimental investigation of aerofoil tonal noise generation," *Journal of Fluid Mechanics*, Vol. 747, 2014, pp. 656–687. https://doi.org/10.1017/jfm.2014.156.

[3] Pröbsting, S., Scarano, F., and Morris, S. C., "Regimes of tonal noise on an airfoil at moderate Reynolds number," *Journal of Fluid Mechanics*, Vol. 780, 2015, pp. 407–438. https://doi.org/10.1017/jfm.2015.475.

[4] Tam, C. K., "Discrete tones of isolated airfoils," *Journal of the Acoustical Society of America*, Vol. 55, No. 6, 1974, pp. 1173–1177. https://doi.org/10.1121/1.1914682.

[5] Wagner, S., Bareiss, R., and Guidata, G., *Wind Turbine Noise*, Springer-Verlag Berlin Heidelberg, Berlin, 1996.

[6] Pröbsting, S., and Yarusevych, S., "Laminar separation bubble development on an airfoil emitting tonal noise," *Journal of Fluid Mechanics*, Vol. 780, 2015, pp. 167–191. https://doi.org/10.1017/jfm.2015.427.

[7] Jaiswal, P., Pasco, Y., Yakhina, G., and Moreau, S., "Experimental investigation of aerofoil tonal noise at low Mach number," *Journal of Fluid Mechanics*, Vol. 932, 2022, pp. 1–31. https://doi.org/10.1017/jfm.2021.1018.

[8] Yakhina, G., Roger, M., Moreau, S., Nguyen, L., and Golubev, V., "Experimental and Analytical Investigation of the Tonal Trailing-Edge Noise Radiated by Low Reynolds Number Aerofoils," *Acoustics*, Vol. 2, No. 2, 2020, pp. 293–329. https://doi.org/10.3390/acoustics2020018.

[9] Nash, E. C., Lowson, M. V., and McAlpine, A., "Boundary-layer instability noise on aerofoils," *Journal of Fluid Mechanics*, Vol. 382, 1999, pp. 27–61. https://doi.org/10.1017/S002211209800367X.

[10] Winkler, J., Wu, H., Moreau, S., Carolus, T., and Sandberg, R. D., "Trailing-edge broadband noise prediction of an airfoil with boundary-layer tripping," *Journal of Sound and Vibration*, Vol. 482, 2020, pp. 1–25. https://doi.org/10.1016/j.jsv.2020.115450.

[11] Paterson, R. W., Vogt, P. G., Fink, M. R., and Munch, C. L., "Vortex noise of isolated airfoils," *Journal of Aircraft*, Vol. 10, No. 5, 1973, pp. 296–302. https://doi.org/10.2514/3.60229.

[12] Fink, M. R., "Prediction of airfoil tone frequencies," *Journal of Aircraft*, Vol. 12, No. 2, 1975, pp. 118–120. https://doi.org/10.2514/3.44421.

[13] Longhouse, R. E., "Vortex shedding noise of low tip speed, axial flow fans," *Journal of Sound and Vibration*, Vol. 53, No. 1, 1977, pp. 25–46. https://doi.org/10.1016/0022-460X(77)90092-X.

[14] Arbey, H., and Bataille, J., "Noise generated by airfoil profiles placed in a uniform laminar flow," *Journal of Fluid Mechanics*, Vol. 134, 1983, pp. 33–47. https://doi.org/10.1017/S0022112083003201.

[15] Desquesnes, G., Terracol, M., and Sagaut, P., "Numerical investigation of the tone noise mechanism over laminar airfoils," *Journal of Fluid Mechanics*, Vol. 591, 2007, pp. 155–182. https://doi.org/10.1017/S0022112007007896.

[16] Schlichting, H., and Gersten, K., *Boundary-Layer Theory*, 9th ed., Springer-Verlag Berlin Heidelberg, 2017.

[17] Kingan, M. J., and Pearse, J. R., "Laminar boundary layer instability noise produced by an aerofoil," *Journal of Sound and Vibration*, Vol. 322, No. 4, 2009, pp. 808–828. https://doi.org/10.1016/j.jsv.2008.11.043.

[18] Deuse, M., and Sandberg, R. D., "Different noise generation mechanisms of a controlled diffusion aerofoil and their dependence on Mach number," *Journal of Sound and Vibration*, Vol. 476, 2020. https://doi.org/10.1016/j.jsv.2020.115317.

[19] Arbey, H., and Bataille, J., "The effect of the leading-edge separation bubble vortex shedding on the far field noise of a Controlled Diffusion airfoil: A DNS study," *Journal of Sound and Vibration*, Vol. 618, 2025, p. 119336. https://doi.org/10.1016/j.jsv.2025.119336.

[20] Wu, H., Moreau, S., and Sandberg, R. D., "On the noise generated by a controlled-diffusion aerofoil at Rec=1.5×10^5," *Journal of Sound and Vibration*, Vol. 487, 2020, p. 115620. https://doi.org/10.1016/j.jsv.2020.115620.

[21] Sanjose, M., Towne, A., Jaiswal, P., Moreau, S., Lele, S., and Mann, A., "Modal analysis of the laminar boundary layer instability and tonal noise of an airfoil at Reynolds number 150,000," *International Journal of Aeroacoustics*, Vol. 18, No. 2-3, 2019, pp. 317–350. https://doi.org/10.1177/1475472X18812798.

[22] Zilstra, A., and Johnson, D. A., "Large Eddy Simulation of Transitional Separated Flow Over a Low Reynolds Number Cambered Airfoil," *Journal of Fluids Engineering*, Vol. 145, 2023. https://doi.org/10.1115/1.4056280.

[23] Zilstra, A., and Johnson, D. A., "Transient Development of a Laminar Separation Bubble Over a Low Reynolds Number Airfoil," *Journal of Fluids Engineering*, Vol. 148, No. 4, 2026. https://doi.org/10.1115/1.4070836.

[24] Zilstra, A., and Johnson, D. A., "Computational Aeroacoustic Prediction of Tonal Noise for Low Reynolds Number Airfoils," *30th AIAA/CEAS Aeroacoustics Conference*, 2024, pp. 1–16. https://doi.org/10.2514/6.2024-3362.

[25] Selig, M. S., Donovan, J. F., and Fraser, D. B., *Airfoils at Low Speeds*, SoarTech Publications, VA, 1989. https://m-selig.ae.illinois.edu/uiuc_lsat/Airfoils-at-Low-Speeds.pdf.

[26] Selig, M. S., Lyon, C. A., Giguere, P., Ninham, C. P., and Guglielmo, J., *Summary of low-speed airfoil data, Vol. 2*, SoarTech Publications, VA, 1996. https://m-selig.ae.illinois.edu/uiuc_lsat/Low-Speed-Airfoil-Data-V2.pdf.

[27] Ghorbanishohrat, F., "Study of a low Re airfoil considering laminar separation bubbles in static and pitching motion," Ph.D. thesis, University of Waterloo, 2019. http://hdl.handle.net/10012/14428.

[28] Tam, N., "An Aeroacoustic Study of Airfoil Self-Noise for Wind Turbine Applications," Master's thesis, University of Waterloo, 2017. http://hdl.handle.net/10012/11736.

[29] Tam, C. K., "Computational aeroacoustics: An overview of computational challenges and applications," *International Journal of Computational Fluid Dynamics*, Vol. 18, No. 6, 2004, pp. 547–567. https://doi.org/10.1080/10618560410001673551.

[30] Graham, "Digital Research Alliance of Canada," 2024. https://alliancecan.ca/en.

[31] Smith, T. A., and Ventikos, Y., "Boundary layer transition over a foil using direct numerical simulation and large eddy simulation," *Physics of Fluids*, Vol. 31, No. 12, 2019. https://doi.org/10.1063/1.5126663.

[32] Thomareis, N., and Papadakis, G., "Effect of trailing edge shape on the separated flow characteristics around an airfoil at low Reynolds number A numerical study," *Physics of Fluids*, Vol. 29, No. 1, 2017. https://doi.org/10.1063/1.4973811.

[33] Galbraith, M. C., and Visbal, M. R., "Implicit large eddy simulation of low-Reynolds-number transitional flow past the SD7003 airfoil," *46th AIAA Aerospace Sciences Meeting and Exhibit*, 2008. https://doi.org/10.2514/6.2010-4737.

[34] Breuer, M., "Effect of Inflow Turbulence on an Airfoil Flow with Laminar Separation Bubble: An LES Study," *Flow, Turbulence and Combustion*, Vol. 101, No. 2, 2018, pp. 433–456. https://doi.org/10.1007/s10494-017-9890-2.

[35] Lobo, B. A., Schaffarczyk, A. P., and Breuer, M., "Investigation into boundary layer transition using wall-resolved large-eddy simulations and modeled inflow turbulence," *Wind Energy Science*, Vol. 7, No. 3, 2022, pp. 967–990. https://doi.org/10.5194/wes-7-967-2022.

[36] Christophe, J., Anthoine, J., and Moreau, S., "Trailing edge noise of a controlled-diffusion airfoil at moderate and high angle of attack," *15th AIAA/CEAS Aeroacoustics Conference*, , No. May, 2009, pp. 11–13. https://doi.org/10.2514/6.2009-3196.

[37] ANSYS Academic Research, Release 20.2, "ANSYS Fluent Theory Guide," *ANSYS Help System*, ANSYS Inc., Release 20.2, 20th ed.

[38] Lang, M., Rist, U., and Wagner, S., "Investigations on controlled transition development in a laminar separation bubble by means of LDA and PIV," *Experiments in Fluids*, Vol. 36, No. 1, 2004, pp. 43–52. URL http://link.springer.com/10.1007/s00348-003-0625-x, https://doi.org/10.1007/s00348-003-0625-x.

[39] McAuliffe, B. R., and Yaras, M. I., "Separation-Bubble-Transition Measurements on a Low-Re Airfoil Using Particle Image Velocimetry," *Volume 3: Turbo Expo 2005, Parts A and B*, Vol. 3, ASME, 2005, pp. 1029–1038. URL https://asmedigitalcollection.asme.org/GT/proceedings/GT2005/47268/1029/312911, https://doi.org/10.1115/GT2005-68663.

[40] Williams, J. E. F., and Hall, L. H., "Aerodynamic sound generation by turbulent flow in the vicinity of a scattering half plane," *Journal of Fluid Mechanics*, Vol. 40, No. 4, 1970, p. 657–670. https://doi.org/10.1017/S0022112070000368.

[41] Saric, W. S., and Tomas, A. S. W., "Experiments on the subharmonic route to turbulence in boundary layers," *Turbulence choatic Phenomena in Fluids; Proceedings of the International Symposium*, Elsevier, Kyoto, Japan, 1984, pp. 117–122.

[42] White, F. M., *Viscous Fluid Flow*, 2nd ed., McGraw Hill, New York, 1991.